Nonlinear Dyn (2016) 85:693–698
DOI 10.1007/s11071-016-2702-8

COMMENTARY

Comments on "Design of α-filter based UDE controllers considering finite control bandwidth"

Alon Kuperman

Received: 2 August 2015 / Accepted: 22 February 2016 / Published online: 4 March 2016

Abstract In the paper "Design of α-filter based UDE controllers considering finite control bandwidth" by A. Kuperman (Nonlinear Dynamics, vol. 81, no. 1, July. 2015), performances of a new first-order α-filter for uncertainty and disturbance estimator (UDE)-based control and a classical first-order UDE filter where examined. It was shown that performance superiority of the α-filter is not straightforward and takes place for limited operating region only in case practical implementation issues of the filters are taken into account. The purpose of this note is complementing (Kuperman in Nonlinear Dyn 81:411–416, 2015) by proving that in case practical implementation restrictions are extended to the overall control system and classical UDE-filter-based controller would always outperform the α-filter-based controller in terms of disturbance and noise rejection, while the α-filter-based controller would be superior in terms of stability.

Keywords Uncertainty and disturbance estimator (UDE) · Robust nonlinear control · UDE filter · Control bandwidth

A. Kuperman (✉)
Hybrid Energy Sources Laboratory, Department of Electrical Engineering and Electronics, Ariel University, POB 3, 40700 Ariel, Israel
e-mail: alonku@ariel.ac.il

1 Introduction

Consider a class of nonlinear dynamical systems described by (all the variables are given in time domain unless stated differently)

$$\begin{aligned}\dot{x} &= \left(-\bar{f} + \Delta f\right) x + \left(\bar{g} + \Delta g\right) u + n \\ &= -\bar{f}x + \bar{g}\left(u + d\right), \end{aligned} \tag{1}$$

where x, u and n represent the state, control input and external non-measurable disturbance, respectively. Moreover, $\bar{f} \geq 0, \bar{g} > 0$ denote nominal (known) constant part of the system, while $\Delta f, \Delta g$ represent corresponding (possibly time-varying, state-dependent and control-dependent) uncertainties. Scalar notations are utilized for simplicity; yet the obtained results may be extended to vector-matrix cases as well. The uncertainty- and disturbance-related terms are lumped into single variable d as

$$d = \bar{g}^{-1}\left(\Delta f x + \Delta g u + n\right). \tag{2}$$

Applying the feedback linearizing control law,

$$u = \bar{g}^{-1}\left(\bar{f}x - Ax + Br\right) - d \tag{3}$$

with r denoting the reference command to the system and $A > 0, B > 0$ determining the desired stable closed-loop dynamics, would bring the closed-loop system to the form of ($A = B$ is a typical case)

$$\dot{x} = -Ax + Br. \tag{4}$$

Nevertheless, (3) cannot be applied as is since the lumped uncertainty and disturbance d is unknown. Note that according to (1),

$$d = \bar{g}^{-1}\left(\dot{x} + \bar{f}x\right) - u. \tag{5}$$

Obviously, (5) cannot be used in (3) as is. UDE-based approach proposes to estimate d as

$$\tilde{d} = d * h = \left(\bar{g}^{-1}\left(\dot{x} + \bar{f}x\right) - u\right) * h, \tag{6}$$

where $h(t)$ is an impulse response of a frequency-selective filter and '*' denotes the convolution operator. Then, $\tilde{d}$ is used in (3) instead of d. The modified control law is therefore

$$u = \bar{g}^{-1}\left(\bar{f}x - Ax + Br\right) - \tilde{d} = \bar{g}^{-1}\left(\bar{f}x - Ax + Br\right) - \left(\bar{g}^{-1}\left(\dot{x} + \bar{f}x\right) - u\right) * h. \tag{7}$$

Rearranging (7), the UDE-based control law is given by

$$u = \bar{g}^{-1}\left(\bar{f}x - L^{-1}\left\{\frac{sH(s)}{1 - H(s)}\right\} * x + L^{-1}\left\{\frac{1}{1 - H(s)}\right\} * (-Ax + Br)\right), \tag{8}$$

where $L\{\cdot\}$ is the Laplace transform operator and $H(s) = L\{h(t)\}$. Substituting (7) into (1) and rearranging results in the following closed-loop dynamics,

$$\dot{x} = -Ax + Br + d - d * h, \tag{9}$$

Taking Laplace transform and rearranging, there is

$$X(s) = T_R(s)R(s) + T_D(s)D(s), \tag{10}$$

where

$$T_R(s) = BT_A(s),\ T_D(s) = T_A(s)T_H(s), \tag{11a}$$

with

$$T_A(s) = (s + A)^{-1},\ T_H(s) = 1 - H(s), \tag{11b}$$

and $X(s) = L\{x(t)\}$, $R(s) = L\{r(t)\}$, $D(s) = L\{d(t)\}$ and $H(s) = L\{h(t)\}$. According to (10), bringing $T_D(s)$ as close to zero as possible allows nearly perfect tracking. Since A is designed according to desired transient performance and $\bar{f}$ denotes the nominal part of the system, $T_D(s)$ can be shaped by proper selection of $H(s)$.

2 Selection of $H(s)$

Consider a first-order α-filter given by [2]

$$H(s) = \frac{(1 - \alpha)s + \omega_T}{s + \omega_T}, \tag{12}$$

with $0 < \alpha < 1$. Then,

$$T_H(s) = \frac{\alpha s}{s + \omega_T}, \tag{13}$$

and

$$T_D(s) = \alpha\frac{s}{(s + \omega_T)(s + A)}. \tag{14}$$

It should be emphasized that classical UDE-filter-based case obeys (12)–(14) for $\alpha = 1$. Note that (14) represents a band-pass filter, i.e. $T_D(0) = T_D(\infty) = 0$. In order to determine peaking frequency and corresponding magnitude of T_D, letting

$$\left(\frac{d}{d\omega}|T_D(\omega)|\right)_{\omega=\omega_{DM}} = 0, \tag{15}$$

results in

$$\omega_{DM} = \sqrt{\omega_T A},\ |T_D(\omega_{DM})| = \frac{\alpha}{\omega_T + A}, \tag{16}$$

indicating that in order to improve the uncertainty/disturbance rejection capability, either ω_T should be increased (cf. Fig. 1) or α should be decreased (cf. Fig. 2). In practical cases, where available control bandwidth is always limited (by e.g. sampling frequency, switching frequency, actuator bandwidth etc.), neither ω_T can be increased to infinity nor α can be decreased to zero. The following section demonstrates that in any practical case (i.e. for a finite control bandwidth), increasing ω_T should be preferred over decreasing α since the former leads to better disturbance rejection.

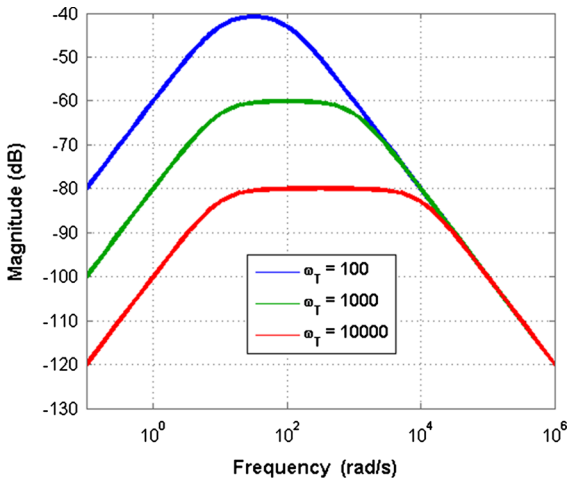

Fig. 1 Influence of ω_T on $|T_D(\omega)|$ for $A = 100$ and $\alpha = 1$

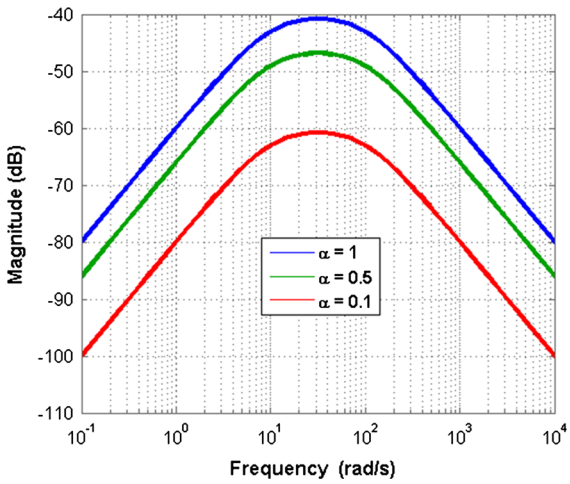

Fig. 2 Influence of α on $|T_D(\omega)|$ for $A = 100$ and $\omega_T = 100$

3 Performance analysis

Substituting (12) in (8) and rearranging, the UDE-based control law is given in Laplace domain by

$$\begin{aligned} U(s) &= -\bar{g}^{-1}\frac{(1-\alpha)s^2+\left(-\bar{f}\alpha+\omega_T+A\right)s+A\omega_T}{\alpha s}X(s) \\ &\quad +\bar{g}^{-1}\frac{B\,(s+\omega_T)}{\alpha s}R(s) \\ &= -H_{FB}(s)X(s)+H_{FF}(s)R(s). \end{aligned} \tag{17}$$

On the other hand, the Laplace transform of the plant (1) is expressed as

$$X(s) = T_f(s)\left(U(s)+D(s)\right), \tag{18}$$

with

$$T_f(s) = \bar{g}\left(s+\bar{f}\right)^{-1}. \tag{19}$$

The overall system is shown in Fig. 3, demonstrating its two-degrees-of-freedom nature [3].

Tracking and disturbance rejection capabilities of the system, given by (10), are then linked to Fig. 3 as

$$T_R(s) = H_{FF}(s)\frac{T_f(s)}{1+T_f(s)H_{FB}(s)}, \tag{20}$$

and

$$T_D(s) = \frac{T_f(s)}{1+T_f(s)H_{FB}(s)}, \tag{21}$$

respectively.

Denote the available control bandwidth as ω_C. Then, $A \leq \omega_C$ must be satisfied in order to achieve the desired tracking performance. On the other hand, in order to assure decent disturbance rejection, the loop gain $L(s) = T_f(s)H_{FB}(s)$ should be higher than unity within the control bandwidth while satisfying $|L(j\omega_C| \leq 1/\sqrt{2}$ in order to respect the available control bandwidth. Moreover, the loop gain determines system stability as well. Taking into account (17) and (19), the loop gain is given by

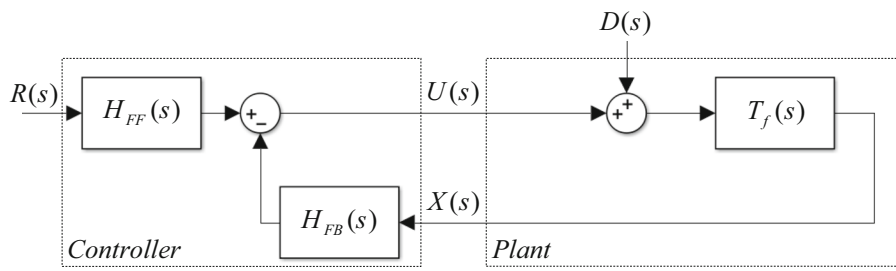

Fig. 3 The overall system in Laplace domain

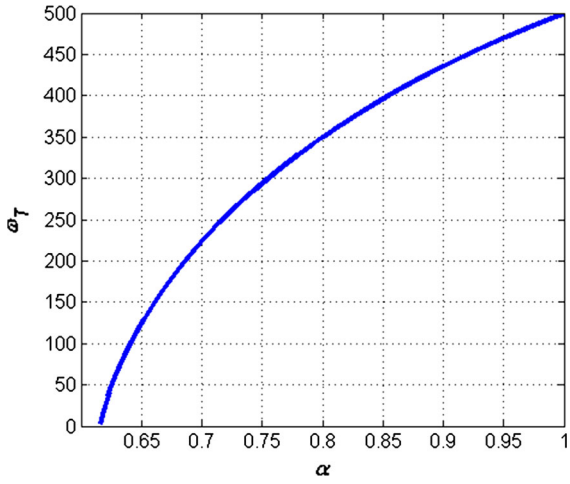

Fig. 4 $\alpha - \omega_T$ trade-off for $\bar{f} = 0$, $A = 200$ and $\omega_C = 1000$

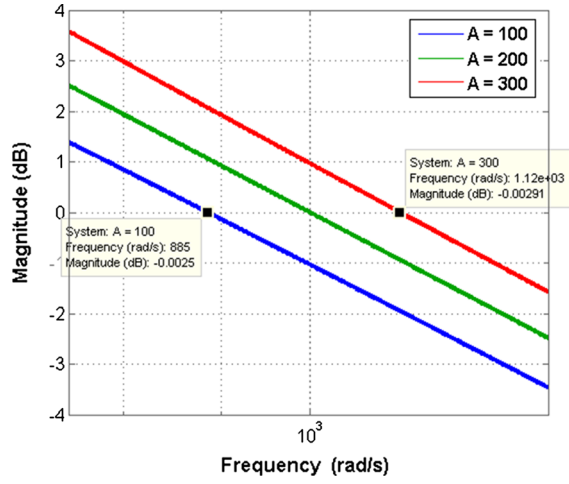

Fig. 6 Influence of A on the loop gain magnitude for $\omega_T = 1000$ and $\bar{f} = 200$

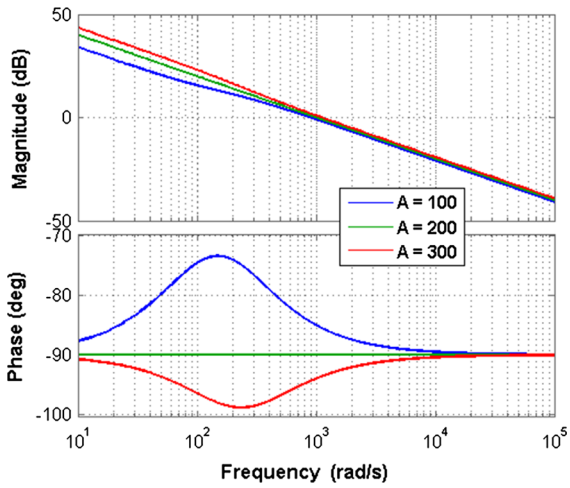

Fig. 5 Influence of A on the loop gain Bode diagram for $\omega_T = 1000$ and $\bar{f} = 200$

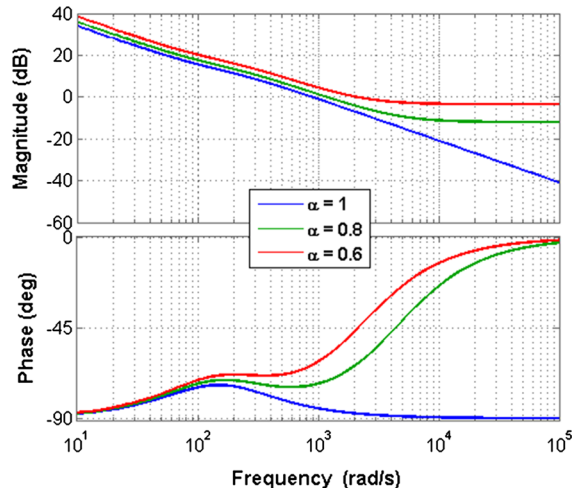

Fig. 7 Influence of α on the loop gain Bode diagram for $\omega_T = 1000$, $\bar{f} = 200$ and $A = 100$

$$L(s) = \frac{(1-\alpha)s^2 + \left(-\bar{f}\alpha + \omega_T + A\right)s + A\omega_T}{\alpha s\left(s + \bar{f}\right)}. \tag{22}$$

Hence, it should satisfy the following inequality,

$$\left|\frac{A\omega_T - (1-\alpha)\omega_C^2 + j\left(-\bar{f}\alpha + \omega_T + A\right)\omega_C}{j\alpha\omega_C\left(j\omega_C + \bar{f}\right)}\right| \leq \frac{1}{\sqrt{2}} \Rightarrow \left(A^2 + \omega_C^2\right)\omega_T^2 + 2\omega_C^2\alpha\left(A - \bar{f}\right)\omega_T + \left((1-\alpha)^2 - \frac{\alpha^2}{2}\right)\omega_C^4 + \omega_C^2\left(\left(A - \bar{f}\alpha\right)^2 - \frac{\alpha^2}{2}\bar{f}^2\right) \leq 0. \tag{23}$$

The solution of (23) would reveal the connection between α and ω_T for a given set of A, $\bar{f}$ and ω_C. The solution is cumbersome and is not listed for brevity. It is only noted that increasing α leads to decreasing ω_T and vice versa. Fig. 4 demonstrates the α - ω_T trade-off for $\bar{f} = 0$, $A = 200$ and $\omega_C = 1000$. On the other hand, considering the classical UDE filter case, i.e.

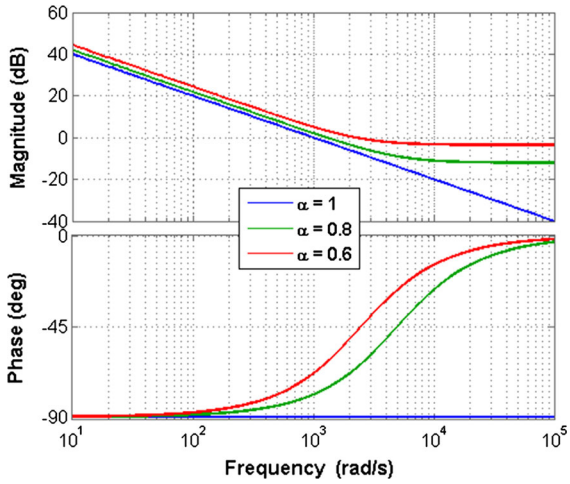

Fig. 8 Influence of α on the loop gain Bode diagram for $\omega_T = 1000$, $\bar{f} = 200$ and $A = 200$

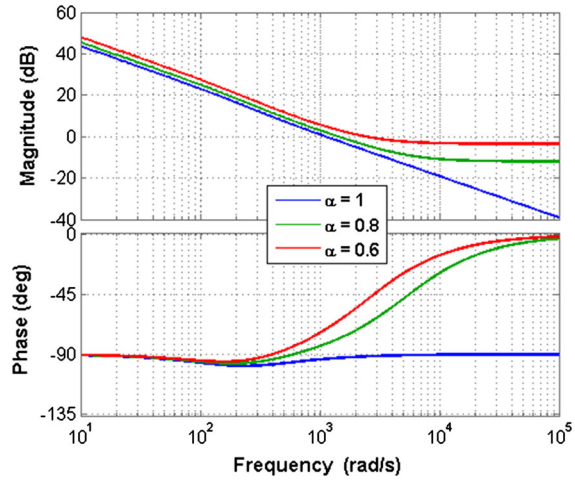

Fig. 9 Influence of α on the loop gain Bode diagram for $\omega_T = 1000$, $\bar{f} = 200$ and $A = 300$

$$L(s)|_{\alpha=1} = \frac{\left(\omega_T + A - \bar{f}\right) s + A\omega_T}{s\left(s + \bar{f}\right)} = \frac{A\omega_T \bar{f}^{-1}}{s} \cdot \frac{\frac{s}{A\omega_T\left(\omega_T + A - \bar{f}\right)^{-1}} + 1}{\frac{s}{\bar{f}} + 1}, \quad (24)$$

allows to obtain an elegant solution of (23), given by

$$\omega_T \leq \omega_C \sqrt{\frac{\left(\frac{1}{2}\right)\omega_C^2 - \left(\left(A - \bar{f}\right)^2 - \frac{1}{2}\bar{f}^2\right)}{A^2 + \omega_C^2}}. \quad (25)$$

It is interesting to note that if $A = \bar{f}$, then

$$L(s)|_{\alpha=1, A=\bar{f}} = \frac{\omega_T}{s}, \quad (26)$$

with

$$\omega_T \leq \frac{\omega_C}{\sqrt{2}}, \quad (27)$$

i.e., the system bandwidth is ω_T, the phase margin is 90° and gain margin is infinite. In case $A > \bar{f}$, the crossover frequency increases, while phase margin decreases. Alternatively, if $A < \bar{f}$, the crossover frequency reduces while phase margin increases. The three cases are shown in Figs. 5 and 6. Next, consider the general case of (22) with $\alpha < 1$. Figs. 7, 8, 9 demonstrate corresponding Bode diagrams for different values of α. It may be concluded that decreasing α improves both disturbance rejection (by increasing the loop gain magnitude) and stability (by increasing the phase margin).

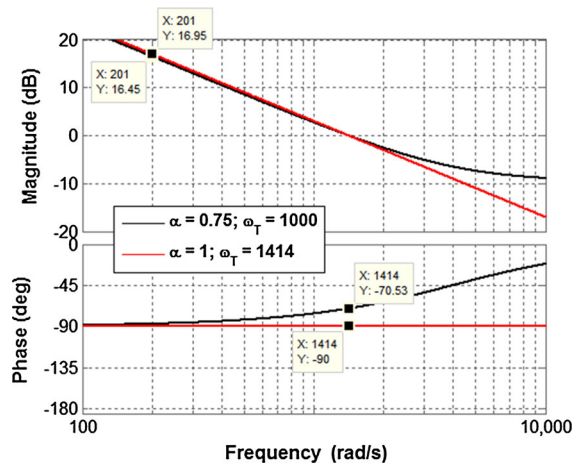

Fig. 10 Comparison of α-filter and UDE-filter-based loop gains

Nevertheless, performance enhancement is achieved at the expense of increased control bandwidth. Note that if control bandwidth increase is possible, ω_T could be increased instead of decreasing α. As an example, consider for simplicity the $A = \bar{f}$ case with $\omega_T = 1000$ and $\alpha = 0.75$, leading to the crossover frequency of 1414.2 rad/s and phase margin of 109.5°. Selecting a classical UDE filter ($\alpha = 1$) with $\omega_T = 1414.2$ leads to a similar crossover frequency with phase margin of 90°. The magnitude of the UDE-filter-based loop gain remains circa 0.5 dB above the magnitude of the

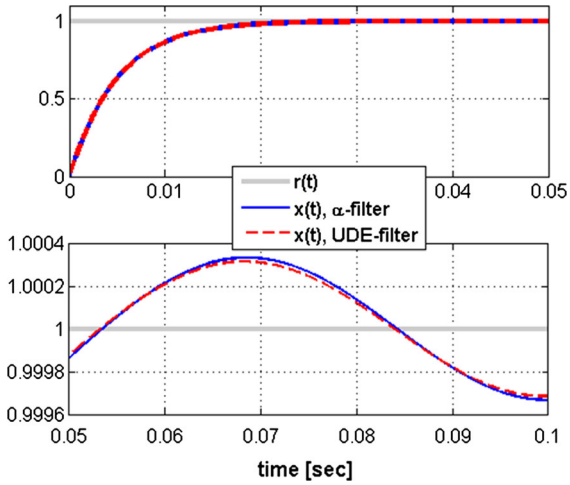

Fig. 11 Time-domain simulation results

α-filter-based loop gain throughout the available bandwidth, as shown in Fig. 10. Consequently, for the same control bandwidth, the α-filter outperforms the UDE filter in terms of stability but is inferior to the UDE filter in terms of disturbance rejection. In addition, while the roll-off of the UDE filter remains -20dB/dec beyond the crossover frequency, the roll-off of the α-filter increases, indicating worse high-frequency noise rejection capabilities. Similar behavior is shown by arbitrary varying A, $\bar{f}$ and ω_T (not shown for brevity).

Time-domain simulation results corresponding to Fig. 10 are shown in Fig. 11 for $r(t) = u(t)$ and $d(t) = \sin(100t)$. While the tracking of both systems is identical, steady-state disturbance rejection of the system based on the UDE filter is slightly better than the one based on the α-filter.

References

1. Kuperman, A.: Design of α-filter based UDE controllers considering finite control bandwidth. Nonlinear Dyn. **81**, 411–416 (2015)
2. Chandar, T.S., Talole, S.E.: Improving the performance of UDE-based controller using a new filter design. Nonlinear Dyn. **77**, 753–768 (2014)
3. Zhong, Q.-C., Kuperman, A., Stobart, R.K.: Design of UDE-based controllers from their two-degree-of-freedom nature. Int. J. Robust Nonl. Control. **21**, 1994–2008 (2011)